International Journal of Electrical, Electronic and Communication Sciences
ISSN: 2517-9438
Vol:14, No:11, 2020

Semi-Analytic Method in Fast Evaluation of Thermal Management Solution in Energy Storage System

Ya Lv

***Abstract*—**This article presents the application of the semi-analytic method (SAM) in the thermal management solution (TMS) of the energy storage system (ESS). The TMS studied in this work is fluid cooling. In fluid cooling, both effective heat conduction and heat convection are indispensable due to the heat transfer from solid to fluid. Correspondingly, an efficient TMS requires a design investigation of the following parameters: fluid inlet temperature, ESS initial temperature, fluid flow rate, working c rate, continuous working time, and materials properties. Their variation induces a change of thermal performance in the battery module, which is usually evaluated by numerical simulation. Compared to complicated computation resources and long computation time in simulation, the SAM is developed in this article to predict the thermal influence within a few seconds. In SAM, a fast prediction model is reckoned by combining numerical simulation with theoretical/empirical equations. The SAM can explore the thermal effect of boundary parameters in both steady-state and transient heat transfer scenarios within a short time. Therefore, the SAM developed in this work can simplify the design cycle of TMS and inspire more possibilities in TMS design.

***Keywords*—**Semi-analytic method, fast prediction model, thermal influence of boundary parameters, energy storage system.

I. Introduction

With increased demand of energy resources, traditional energy solution unavoidably induces non-neglected ecology issues, such as smog and killed-nature lives. Therefore, renewable energy is up-rising in the market, as shown in Fig. 1 [1] in which Denmark is leading development of renewable energy, and other countries are on the way of catching up. To enhance and complement application of Wind Energy and Solar Energy, ESS is indispensable by balancing influence of intermittent weather conditions. Moreover, ESS plays important role in Microgrids development, as displayed in Fig. 2 [2]. ESS can function to shave peak and regulate frequency of grid, as well as provide uninterrupted power supply or black-start at off-grid situations.

Mainstream ESS is composed of Lithium-ion battery cells. Lithium-ion battery's performance is represented by major five indicators: capacity, working c-rate, cycle life, cost and safety. They are influenced by many factors, among which temperature is the most crucial. Lithium-ion battery favors temperature range of 15 °C to 35 °C, too low or too high temperature shortens battery lifecycle by increasing internal resistance, correspondingly, degrades capacity and weakens safety [3], [4]. As a result, an effective TMS is significant in maintaining of battery's performance and extension of battery's lifecycle. TMS exploration involves a number of trials, where the SAM is needed to simplify design cycle and inspire more design possibilities.

Ya LV is with the Durapower Group, Singapore (e-mail: laylaneylv@gmail.com).

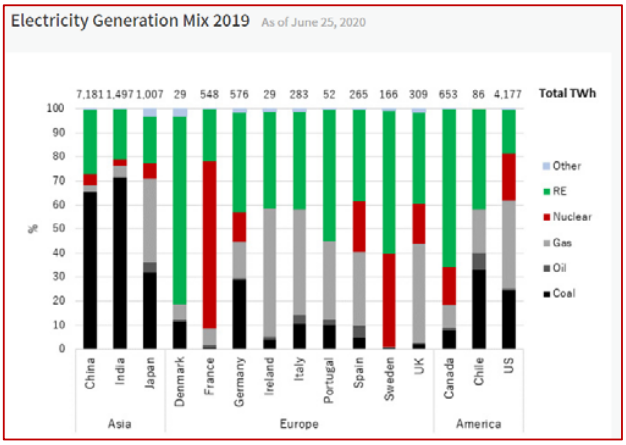

Fig. 1 Electricity generation in different countries [1]

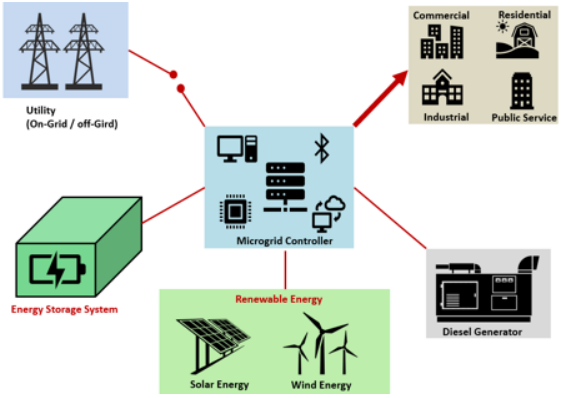

Fig. 2 Microgrids development

II. Methodology

A module design of ESS is investigated in this work, in which heat generated by battery cells will be conducted and spread to cooling surface, to be taken away by the flowing fluid, as shown in Fig. 3. The thermal network [5] of this ESS is described in Fig. 4, in which two major thermal barriers are indicated, one is between battery cells and cooling surface R_{th1}, the other is between cooling surface and flowing fluid R_{th2}. In this work, we assume there is thermal interfacial materials and heat spreading structure in the module, so R_{th2}. dominates the module's thermal performance.

TABLE I
NOMENCLATURE

$R_{th,i}$	Thermal resistance	$C_{th,i}$	Heat capacity	$Z_{th,i}$	Thermal impedance
t	Time	q_{tot}	Total heat power	Nu	Nusselt number
h_{conv}	Convective coefficient	k_{fluid}	Fluid thermal conductivity	Re	Reynold number
Pr	Prandtl number	v_{fluid}	Fluid kinetic viscosity	$A_{cooling}$	Cooling area
D	Characteristic length	U	Fluid velocity	$\dot{m}_{fluid}$	Mass flowrate
$A_{cross-section}$	Cross-sectional area of fluid duct	ρ_{fluid}	Fluid density	T_{cell}	Battery cell temperature
$T_{hottest\ cell}$	Max temperature of hottest cell	$T_{coldest\ cell}$	Max temperature of coldest cell	q_{flow}	Heat power dissipated to fluid
T_{fluid}^{outlet}	Fluid outlet average temperature	T_{fluid}^{inlet}	Fluid inlet average temperature	$\overline{T_{fluid}}$	Fluid average temperature
m_{cell}	Mass of battery cells	E_{cell}	Thermal energy absorbed by battery cells	T_{cell}^{0}	Initial temperature of battery cells

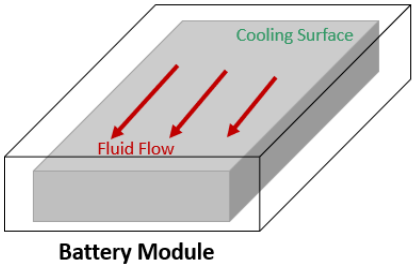

Fig. 3 Lithium-ion battery module

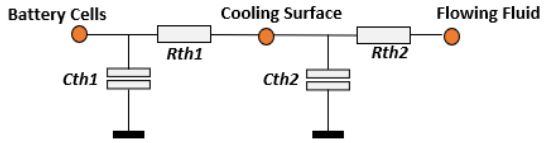

Fig. 4 Thermal network of fluid-cooling ESS

In the studied battery module, change of $\dot{m}_{fluid}$ affects heat convection between fluid and cooling surface, namely, R_{th2}. In heat transfer, R_{th2} can be calculated with empirical equations, as shown in (1)-(8) [6] in which Nu is the ratio of fluid conduction thermal resistance to fluid convective thermal resistance at solid-fluid boundary, Re is calculated with fluid velocity and flow duct characteristic length, Pr is determined by fluid type. Via the equations, R_{th2} can be calculated by obtaining h_{conv} from Nu, before which, the Re is estimated for selecting solving empirical equation. Consequently, there will be an updated R_{th2} when $\dot{m}_{fluid}$ varies.

The average Nu _ empirical equations:

$$Nu = 0.664\, Re_L^{0.5} Pr^{1/3}, \qquad Re < 5 * 10^5 \tag{1}$$

$$Nu = 0.037\, Re_L^{0.8} Pr^{1/3},\ 5 * 10^5 \le Re \le 10^8, 0.6 \le Pr \le 60 \tag{2}$$

$$Nu = \frac{h_{conv} D}{k_{fluid}},\ Re = \frac{UD}{v_{fluid}} \tag{3}$$

$$R_{th2} = 1/(h_{conv} A_{cooling}) \tag{4}$$

$$\dot{m}_{fluid} = \rho_{fluid} U A_{cross-section} \tag{5}$$

$$\frac{R_{th2-1}}{R_{th2-0}} = \frac{h_{conv-0}}{h_{conv-1}} = \frac{Nu_0}{Nu_1} \tag{6}$$

$$\frac{Nu_0}{Nu_1} = \left(\frac{Re_0}{Re_1}\right)^{0.5} = \left(\frac{\dot{m}_{fluid-0}}{\dot{m}_{fluid-1}}\right)^{0.5}, \qquad Re < 5 * 10^5 \tag{7}$$

$$\frac{Nu_0}{Nu_1} = \left(\frac{Re_0}{Re_1}\right)^{0.8} = \left(\frac{\dot{m}_{fluid-0}}{\dot{m}_{fluid-1}}\right)^{0.8}, \qquad 5 * 10^5 \le Re \le 10^8 \tag{8}$$

III. Steady-State Analysis

Steady-state heat transfer is non-relevant with time or heat capacity. Thus, (9)-(13) [7] can be applied to describe the heat transfer in the battery module, the heat power will be transferred to flowing fluid for its thermal absorption.

$$q_{tot} = \frac{T_{hottest\ cell} - \overline{T_{fluid}}}{R_{tot}^{max}} = \frac{T_{coldest\ cell} - \overline{T_{fluid}}}{R_{tot}^{min}} \tag{9}$$

$$q_{tot} = \dot{m}_{fluid} * C_{fluid} * (T_{fluid}^{outlet} - T_{fluid}^{inlet}) \tag{10}$$

$$R_{tot} = R_{th1} + R_{th2} \tag{11}$$

$$\overline{T_{fluid}} = (T_{fluid}^{inlet} + T_{fluid}^{outlet})/2 \tag{12}$$

$$\Delta T_{cells}^{max} = T_{hottest\ cell} - T_{coldest\ cell} \tag{13}$$

By correlating numerical simulation with theoretical/ empirical equations, the SAM can forecast thermal influence at varied input parameters. Fig. 5 shows the SAM flowchart in steady-state analysis, in which thermal simulation of battery module can be conducted at input parameters: $T_{fluid}^{inlet}, \dot{m}_{fluid}, q_{tot}$. Then, R_{tot}^{max}, R_{tot}^{min} will be calculated from simulation results based on (9). If $\dot{m}_{fluid}$ changes, R_{tot}^{max}, R_{tot}^{min} need to be updated on basis of (7) or (8). According to (9)-(13), the thermal effect of varied $T_{fluid}^{inlet}/\dot{m}_{fluid}/q_{tot}$ can be predicted by updating $T_{hottest\ cell}$, ΔT_{cells}^{max} in battery module.

A. Steady-State Case Study

In this steady-state analysis, seven cases were studied, as shown in Table II in which a reference case was simulated to be used in SAM, the other six cases were investigated via simulation and SAM respectively. It is found in Table II that: T_{fluid}^{inlet} changes in case1 and 2, $\dot{m}_{fluid}$ varies in case3 and 4, case5 and 6 reflects change of q_{tot}. In Table III,, the R_{tot}^{max}, R_{tot}^{min} obtained from simulation results of reference case can be found. Table IV lists comparison of updated R_{tot}^{max}, R_{tot}^{min} between simulation and SAM based on $\dot{m}_{fluid}$ variation in case3 and 4. Comparison of $T_{hottest\ cell}$, ΔT_{cells}^{max} between

simulation and SAM on six studied cases is indicated in Table V.

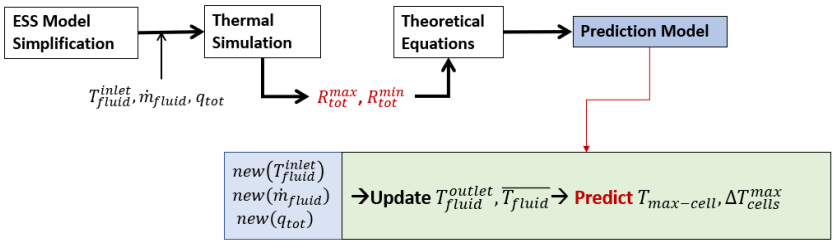

Fig. 5 SAM flow chart in steady-state analysis

TABLE II
WORKING CONDITIONS OF ALL STUDY CASES IN STEADY-STATE ANALYSIS

	T_{fluid}^{inlet}, °C	$\dot{m}_{fluid}$, kg/s	q_{tot}, W
Reference Case	15	0.035	406
Case1	20	0.035	406
Case2	25	0.035	406
Case3	15	0.0175	406
Case4	15	0.0525	406
Case5	15	0.04	306
Case6	15	0.04	206

TABLE III
THERMAL RESISTANCE OBTAINED FROM SIMULATION OF REFERENCE CASE

	R_{tot}^{max}, K/W	R_{tot}^{min}, K/W	$T_{hottest\ cell}$, °C	ΔT_{cells}^{max}, °C
Reference Case	0.055	0.039	43.18	6.45

TABLE IV
UPDATED THERMAL RESISTANCE BASED ON MASS FLOWRATE VARIATION

R_{tot}^{max}, K/W	Case3	Case4	Remark
Thermal Simulation	0.078	0.044	Re was estimated to be < $5 * 10^5$.
SAM	0.0783	0.045	
Relative Difference	0.4%	2.3%	
R_{tot}^{min}, K/W	Case3	Case4	
Thermal Simulation	0.053	0.03	
SAM	0.056	0.032	
Relative Difference	5.7%	6.7%	

TABLE V
COMPARISON OF THERMAL EVALUATION BETWEEN SIMULATION AND SAM

$T_{hottest\ cell}$, °C	Case1	Case2	Case3	Case4	Case5	Case6
Thermal Simulation	48.42	53.62	58.5	36.57	36.04	29.08
SAM	48.24	53.24	58.32	37.2	36.29	29.33
Relative Difference	0.4%	0.7%	0.3%	1.7%	0.7%	0.9%
ΔT_{cells}^{max}, °C	Case1	Case2	Case3	Case4	Case5	Case6
Thermal Simulation	6.51	6.55	10.22	5.32	4.83	3.35
SAM	6.45	6.45	9.12	5.27	4.86	3.27
Relative Difference	0.9%	1.5%	10.7%	1%	0.6%	2.3%

B. Steady-State Results and Discussion

As is seen in Table IV, the relative difference between simulation and SAM is < 3% for R_{tot}^{max}, < 7% for R_{tot}^{min}. This is due to the application of empirical equations (1) and (2) in updating of R_{tot}, correspondingly, we can find relative difference of 10.7% for ΔT_{cells}^{max} in case3, as shown in Table V. But the relative difference between simulation and SAM in other cases is < 3%, as listed in Table V. Therefore, a good matching between simulation and SAM can be found in this steady-state analysis. Compared to tedious simulation work and consumable time, the SAM can instantly predict thermal effect from variation of input parameters in battery module.

IV. TRANSIENT ANALYSIS

Different from steady-state analysis, t, T_{cell}^0, C_{thi} are becoming influential factors in transient heat transfer. So, energy equivalent equation is applied to describe the heat transfer comprehensively, as shown in (17)-(19). In this transient analysis of battery module, we assumed that heat power generated by battery cells is divided into two parts, one part is thermally absorbed by battery cells, the other part is transferred to flowing fluid via cooling surface. Correspondingly, an approximate thermal network can be generated, as shown in Fig. 6.

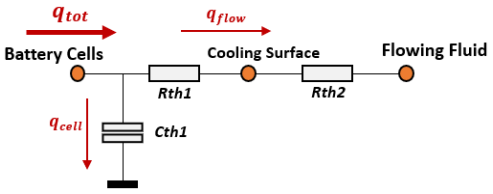

Fig. 6 Approximate thermal network in transient analysis of fluid-cooling ESS

In the SAM, numerical simulation together with theoretical and empirical equations contributes to the thermal prediction. Fig. 7 shows the SAM flowchart in transient analysis, in which thermal simulation of battery module can be conducted at six known parameters $T_{fluid}^{inlet}, \dot{m}_{fluid}, q_{tot}, t, T_{cell}^0, C_{thi}$. Then, R_{th2}^{sim} will be obtained from simulation results based on (14)-(16). When $\dot{m}_{fluid}$ changes, R_{th2}^{sim} will be updated on basis of (7) or (8). Next, the iterative prediction model will work by assuming $T_{fluid}^{outlet}, \overline{T_{fluid-0}}$. The assumed T_{fluid}^{outlet} can be used to calculate T_{cell}^t via (17)-(19), and q_{flow}^t will be calculated via (19). Thereafter, $\overline{T_{fluid-itr}}$ can be obtained from (20) and (21). The difference between $\overline{T_{fluid-itr}}$ and $\overline{T_{fluid-0}}$ will be controlled by iterating the whole prediction process until it falls below a threshold. This is when the predicted T_{cell}^t

can be gained. Because of the iterative prediction process in SAM in transient analysis, only T_{cell}^{t} is forecasted to represent the thermal effect from change of input parameters.

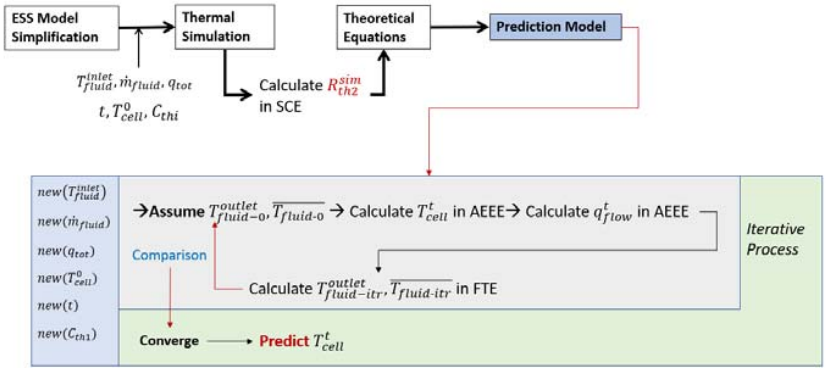

Fig. 7 SAM flow chart in transient analysis

Simulation Calculation Equations (SCE):

$$R_{th2}^{sim} = (T_{cell}^{t-sim} - \overline{T_{fluid-sim}})/q_{flow}^{t-sim} \quad (14)$$

$$q_{flow}^{t-sim} = (q_{tot} * t - E_{cell}^{sim})/t \quad (15)$$

$$E_{cell}^{sim} = m_{cell} * C_{cell} * \left(T_{cell}^{t-sim} - T_{cell}^{0}\right) \quad (16)$$

Approximate Energy Equivalent Equations (AEEE):

$$q_{tot} * t \approx E_{cell}^{t} + q_{flow}^{t} * t \quad (17)$$

$$E_{cell}^{t} = m_{cell} * C_{cell} * (T_{cell}^{t} - T_{cell}^{0}) \quad (18)$$

$$q_{flow}^{t} = (T_{cell}^{t} - \overline{T_{fluid}})/ R_{th2} \quad (19)$$

Fluid Transfer Equation (FTE):

$$q_{flow}^{t} = \dot{m}_{fluid} * C_{fluid} * (T_{fluid}^{outlet} - T_{fluid}^{inlet}) \quad (20)$$

$$\overline{T_{fluid}} = (T_{fluid}^{outlet} + T_{fluid}^{inlet})/2 \quad (21)$$

A. Transient Case Study

In transient analysis, 13 cases were studied, as shown in Table VI. A reference case was simulated to be used in SAM, the other 12 cases were probed via simulation and SAM respectively. From Table VI, it is found that: T_{fluid}^{inlet} changes in case1 and 2, $\dot{m}_{fluid}$ varies in case3 and 4, case5 and 6 reflects change of q_{tot}, variations of T_{cell}^{0}, t, C_{th1} are indicated from case7 to 12. Table VII displays R_{th2}^{sim} obtained from simulation results of reference case. Table VIII lists comparison of updated R_{th2} between simulation and SAM given $\dot{m}_{fluid}$ variation in case3 and 4. Comparison of $T_{hottest\ cell}$ between simulation and SAM in all twelve studied cases is indicated in Table IX.

TABLE VI
WORKING CONDITIONS OF STUDY CASES IN TRANSIENT ANALYSIS

	Tfluidinlet, °C	mfluid, kg/s	qtot, W	Tcell0, °C	t, s	Cth1, J/kg/K
Reference Case	15	0.035	406	20	1800	678
Case1	20	0.035	406	20	1800	678
Case2	25	0.035	406	20	1800	678
Case3	15	0.0175	406	20	1800	678
Case4	15	0.0525	406	20	1800	678
Case5	15	0.035	306	20	1800	678
Case6	15	0.035	206	20	1800	678
Case7	15	0.035	406	30	1800	678
Case8	15	0.035	406	40	1800	678
Case9	15	0.035	406	20	900	678
Case10	15	0.035	406	20	3600	678
Case11	15	0.035	406	20	1800	452
Case12	15	0.035	406	20	1800	1017

TABLE VII
THERMAL RESISTANCE OBTAINED FROM SIMULATION OF REFERENCE CASE

	R_{th2}^{sim}, K/W	$T_{hottest\ cell}$, °C
Reference Case	0.069	32.54

TABLE VIII
UPDATED THERMAL RESISTANCE BASED ON VARIED MASS FLOWRATE

R_{th2}, K/W	Case3	Case4	Remark
Thermal Simulation	0.09	0.056	Re was estimated to be < $5 * 10^5$.
SAM	0.097	0.0563	
Relative Difference	7.7%	0.5%	

TABLE IX
COMPARISON OF THERMAL EVALUATION BETWEEN SIMULATION AND SAM

$T_{hottest\ cell}$, °C	Case1	Case2	Case3	Case4	Case5	Case6
Thermal Simulation	35.04	37.51	34.94	30.73	28.86	25.17
SAM	34.46	36.61	35.27	30.56	28.76	25.20
Relative Difference	1.64%	2.4%	0.95%	0.55%	0.35%	0.11%
$T_{hottest\ cell}$, °C	Case7	Case8	Case9	Case10	Case11	Case12
Thermal Simulation	37.79	42.96	27.72	37.9	35.11	29.96
SAM	38.04	43.75	27.84	37.25	35.22	29.58
Relative Difference	0.66%	1.85%	0.44%	1.71%	0.32%	1.26%

B. Transient Results and Discussion

As is shown in Table VIII, the relative difference between simulation and SAM is < 8% for R_{th2}. This is due to the application of empirical equations (1) and (2) in updating of R_{th2}. In Table IX, it can be found that the relative difference of $T_{hottest\ cell}$ between simulation and SAM in all 12 cases is < 3%. Therefore, a good matching between simulation and SAM is verified in transient analysis of battery module. Given above comparison results between simulation and SAM, it is confident to predict thermal influence from varied input parameters in battery module.

V. Conclusion

The present work introduces SAM applied for predicting thermal influence of varied factors and optimizing TMS in ESS. The SAM is developed on basis of numerical simulation and theoretical/empirical equations. In this work, both steady-state and transient heat transfer were analyzed, thermal effect of varied input parameters was investigated via different cases. In steady-state analysis, an excellent matching was found in six cases between simulation and SAM on predicting $T_{hottest\ cell}$, ΔT_{cells}^{max} in battery module. In transient analysis, an excellent consistency was verified in 12 cases between simulation and SAM on forecasting $T_{hottest\ cell}$ in battery module.

Compared to all-cases numerical simulation, the SAM only needs one simulation of reference-case to be built up in both steady-state and transient scenarios. Compared to consumable computation resources and long computation time in numerical simulation, the SAM can predict thermal impact from changeable boundary parameters within a few seconds. In all, the SAM can be applied to improve TMS design efficiency and predict thermal performance of ESS within short time.

References

[1] https://www.renewable-ei.org/en/statistics/international/.
[2] Dr. V. Gomathy, Dr.S. Sheeba Rani, Dr.K. Sujatha. Soft switched solar integrated power optimizer, International Journal of Pure and Applied Mathematics, Volume 119 No. 12 2018, 1655-1663.
[3] Shuai Ma, Modi Jiang, Peng Tao, Chengyi Song, Jianbo Wu, Jun Wang, Tao Deng, Wen Shang. Temperature effect and thermal impact in lithium-ion batteries: A review, Progress in Natural Science: Materials International Volume 28, Issue 6, December 2018, Pages 653-666.
[4] U. Iraola, I. Aizpuru, J. M. Canales, A. Etxeberria and I. Gil. "Methodology for thermal modelling of lithium-ion batteries," IECON 2013 - 39th Annual Conference of the IEEE Industrial Electronics Society, Vienna, 2013, pp. 6752-6757, doi: 10.1109/IECON.2013.6700250.
[5] https://www.thermal-engineering.org/what-is-laminar-vs-turbulent-nusselt-number-definition/.
[6] Arun Mambazhasseri Divakaran, Dean Hamilton, Krishna Nama Manjunatha and Manickam Minakshi. Design, Development and Thermal Analysis of Reusable Li-Ion Battery Module for Future Mobile and Stationary Applications. Energies 2020, 13, 1477.
[7] Chengtao Lin, Can Cui, Xiaotian Xu. Lithium-ion Battery Electro-thermal Model and Its Application in the Numerical Simulation of Short Circuit Experiment. EVS27 Barcelona, Spain, November 17-20, 2013..